

## Spectral and Raman Analysis of Nd<sup>3+</sup> Doped Zinc Lithium Soda lime Cadmium Borosilicate Glasses

S.L.Meena

Ceramic Laboratory, Department of Physics, Jai Narain Vyas University, Jodhpur 342001(Raj.) India

\*Corresponding Author E-Mail: shankardiya7@rediffmail.com

### Abstract

Glass of the system:  $(35-x) \text{SiO}_2:10\text{ZnO}:10\text{Li}_2\text{O}:10\text{CaO}:10\text{Na}_2\text{O}:10\text{CdO}:15\text{B}_2\text{O}_3: x\text{Nd}_2\text{O}_3$ . (Where  $x=1, 1.5, 2$  mol %) have been prepared by melt-quenching method. The amorphous nature of the glasses was confirmed by X-ray diffraction studies. Optical absorption, Excitation, fluorescence and Raman spectra have been recorded at room temperature for all glass samples. Slater-Condon parameters  $F_k$  ( $k=2, 4, 6$ ), Lande's parameter  $\xi_{4f}$  and Racah parameters  $E^k$  ( $k=1, 2, 3$ ) have been computed. Using these parameters energies and intensities of these bands has been calculated. Judd-Ofelt intensity parameters  $\Omega_\lambda$  ( $\lambda=2, 4, 6$ ) are evaluated from the intensities of various absorption bands of optical absorption spectra. Using these intensity parameters various radiative properties like spontaneous emission probability ( $A$ ), branching ratio ( $\beta_R$ ), radiative life time ( $\tau$ ) and stimulated emission cross-section ( $\sigma_p$ ) of various emission lines have been evaluated.

**Keywords:** ZLCBS Glasses, Optical Properties, Judd-Ofelt Theory, Raman Spectra.

### Introduction:

Rare earth doped phosphate glasses are being extensively studied due to their technological importance and their applications in the field of glass ceramics, thermal and mechanical sensors, reflecting windows [1-5]. Among different host matrices, silicate glasses are quite prone with the advantages such as low non-linear refractive index, good physical and chemical stability and high transparency from near Ultra Violet to mid-Infrared region [6-11]. Due to their good chemical durability, neodymium-doped soda-lime silicate glasses are attractive materials for the fabrication of low-cost integrated optical amplifiers by using the ion-exchange technique. Glasses contain B<sub>2</sub>O<sub>3</sub> have received increased attention due to their application in the field of glass ceramics, reflecting windows, thermal and mechanical sensors [12-14]. The addition of network modifier (NWF) Li<sub>2</sub>O is to improve both electrical and mechanical properties of such glasses. Silicate glasses also exhibit high RE ions solubility [15]. Nd<sup>3+</sup> doped materials have proven to be among the most efficient candidates for photonic devices, such as lasers and planer wave guides [16-20].

In the present work, Optical absorption, Excitation, fluorescence and Raman spectra have been recorded at room temperature for all glass samples. From the spectral data various energy interaction parameters like Slater-Condon parameters  $F_k$  ( $k=2, 4, 6$ ), Lande's parameter  $\xi_{4f}$  and Racah parameters  $E^k$  ( $k=1, 2, 3$ ) have been computed. The Judd-Ofelt theory has been applied to compute the intensity parameters  $\Omega_\lambda$  ( $\lambda=2, 4, 6$ ). To understand the laser efficiency of these materials, the value of spectroscopy quality factor ( $\Omega_4/\Omega_6$ ) has been evaluated.

## Experimental:

### Preparation of glasses:

The following  $\text{Nd}^{3+}$  doped borosilicate glass samples (35-x)  $\text{SiO}_2:10\text{ZnO}:10\text{Li}_2\text{O}:10\text{CaO}:10\text{Na}_2\text{O}:10\text{CdO}:15\text{B}_2\text{O}_3: x\text{Nd}_2\text{O}_3$  (where  $x = 1, 1.5, 2$ ) have been prepared by melt-quenching method. Analytical reagent grade chemical used in the present study consist of  $\text{SiO}_2$ ,  $\text{ZnO}$ ,  $\text{Li}_2\text{O}$ ,  $\text{CaO}$ ,  $\text{Na}_2\text{O}$ ,  $\text{CdO}$ ,  $\text{B}_2\text{O}_3$  and  $\text{Nd}_2\text{O}_3$ . They were thoroughly mixed by using an agate pestle mortar. Then melted at  $1075^\circ\text{C}$  by an electrical muffle furnace for 2 hours. After complete melting, the melts were quickly poured in to a preheated stainless steel mould and annealed at temperature of  $350^\circ\text{C}$  for 2 h to remove thermal strains and stresses. Every time fine powder of cerium oxide was used for polishing the samples. The glass samples so prepared were of good optical quality and were transparent. The chemical compositions of the glasses with the name of samples are summarized in **Table 1**.

**Table 1:** Chemical composition of the glasses

Sample	Glass composition (mol %)
ZLSLCBS (UD)	$35\text{SiO}_2:10\text{ZnO}:10\text{Li}_2\text{O}:10\text{CaO}:10\text{Na}_2\text{O}:10\text{CdO}:15\text{B}_2\text{O}_3:$
ZLSLCBS (ND1)	$34\text{SiO}_2:10\text{ZnO}:10\text{Li}_2\text{O}:10\text{CaO}:10\text{Na}_2\text{O}:10\text{CdO}:15\text{B}_2\text{O}_3:1\text{Nd}_2\text{O}_3$
ZLSLCBS (ND1.5)	$33.5\text{SiO}_2:10\text{ZnO}:10\text{Li}_2\text{O}:10\text{CaO}:10\text{Na}_2\text{O}:10\text{CdO}:15\text{B}_2\text{O}_3:1.5\text{Nd}_2\text{O}_3$
ZLSLCBS (ND2)	$33\text{SiO}_2:10\text{ZnO}:10\text{Li}_2\text{O}:10\text{CaO}:10\text{Na}_2\text{O}:10\text{CdO}:15\text{B}_2\text{O}_3:2\text{Nd}_2\text{O}_3$

ZLSLCBS (UD)-Represents undoped Zinc Lithium Soda lime Cadmium Borosilicate glass specimen.

ZLSLCBS (ND)-Represents  $\text{Nd}^{3+}$  doped Zinc Lithium Soda lime Cadmium Borosilicate glass specimens.

### Theory:

#### Oscillator Strength:

The intensity of spectral lines are expressed in terms of oscillator strengths using the relation [21].

$$f_{\text{expt.}} = 4.318 \times 10^{-9} \int \epsilon(\nu) d\nu \quad (1)$$

where,  $\epsilon(\nu)$  is molar absorption coefficient at a given energy  $\nu$  ( $\text{cm}^{-1}$ ), to be evaluated from Beer–Lambert law.

Under Gaussian Approximation, using Beer–Lambert law, the observed oscillator strengths of the absorption bands have been experimentally calculated [22], using the modified relation:

$$P_m = 4.6 \times 10^{-9} \times \frac{1}{cl} \log \frac{I_0}{I} \times \Delta\nu_{1/2} \quad (2)$$

where,  $c$  is the molar concentration of the absorbing ion per unit volume,  $l$  is the optical path length,  $\log I_0/I$  is optical density and  $\Delta\nu_{1/2}$  is half band width.

#### Judd-Ofelt Intensity Parameters

According to Judd [23] and Ofelt [24] theory, independently derived expression for the oscillator strength of the induced forced electric dipole transitions between an initial  $J$  manifold  $|4f^N(S, L) J\rangle$  level and the terminal  $J'$  manifold  $|4f^N(S', L') J'\rangle$  is given by:

$$\frac{8\pi^2 mc \bar{\nu}}{3h(2J+1)n} \left[ \frac{(n^2+2)^2}{9} \right] \times S(J, J') \quad (3)$$

Where, the line strength  $S(S', L')$  is given by the equation

$$S(J, J') = e^2 \sum_{\lambda} \Omega_{\lambda} \langle 4f^N(S, L) J \| U^{(\lambda)} \| 4f^N(S', L') J' \rangle^2 \quad (4)$$

$\lambda = 2, 4, 6$

In the above equation  $m$  is the mass of an electron,  $c$  is the velocity of light,  $\bar{\nu}$  is the wave number of the transition,  $h$  is Planck's constant,  $n$  is the refractive index,  $J$  and  $J'$  are the total angular momentum of the initial and final level respectively,  $\Omega_{\lambda}$  ( $\lambda = 2, 4, 6$ ) are known as Judd-Ofelt intensity parameters.

### Radiative Properties

The  $\Omega_{\lambda}$  parameters obtained using the absorption spectral results have been used to predict radiative properties such as spontaneous emission probability ( $A$ ) and radiative life time ( $\tau_R$ ), and laser parameters like fluorescence branching ratio ( $\beta_R$ ) and stimulated emission cross section ( $\sigma_p$ ).

The spontaneous emission probability from initial manifold  $|4f^N(S', L') J'\rangle$  to a final manifold  $|4f^N(S, L) J\rangle$  is given by:

$$A[(S', L') J'; (S, L) J] = \frac{64 \pi^2 \bar{\nu}^3}{3h(2J'+1)} \left[ \frac{n(n^2+2)^2}{9} \right] \times S(J', J) \quad (5)$$

$$\text{where, } S(J', J) = e^2 [\Omega_2 \| U^{(2)} \|^2 + \Omega_4 \| U^{(4)} \|^2 + \Omega_6 \| U^{(6)} \|^2]$$

The fluorescence branching ratio for the transitions originating from a specific initial manifold  $|4f^N(S', L') J'\rangle$  to a final manifold  $|4f^N(S, L) J\rangle$  is given by

$$\beta[(S', L') J'; (S, L) J] = \sum \frac{A[(S', L') J'; (S, L) J]}{A[(S', L') J'; (\bar{S}, \bar{L}) \bar{J}]} \quad (6)$$

$S, L, J$  where, the sum is over all terminal manifolds.

The radiative life time is given by

$$\tau_{\text{rad}} = \sum A[(S', L') J'; (S, L) J] = A_{\text{Total}}^{-1} \quad (7)$$

$S, L, J$  where, the sum is over all possible terminal manifolds. The stimulated emission cross-section for a transition from an initial manifold  $|4f^N(S', L') J'\rangle$  to a final manifold  $|4f^N(S, L) J\rangle$  is expressed as

$$\sigma_p(\lambda_p) = \left[ \frac{\lambda_p^4}{8\pi c n^2 \Delta\lambda_{\text{eff}}} \right] \times A[(S', L') J'; (\bar{S}, \bar{L}) \bar{J}] \quad (8)$$

where,  $\lambda_p$  the peak fluorescence wavelength of the emission band and  $\Delta\lambda_{\text{eff}}$  is the effective fluorescence line width.

### Nephelauxetic Ratio ( $\beta$ ) and Bonding Parameter ( $b^{1/2}$ )

The nature of the R-O bond is known by the Nephelauxetic Ratio ( $\beta$ ) and Bonding

Parameters ( $b^{1/2}$ ), which are computed by using following formulae [25, 26]. The Nephelauxetic Ratio is given by

$$\beta' = \frac{\nu_g}{\nu_a} \quad (9)$$

where,  $\nu_a$  and  $\nu_g$  refer to the energies of the corresponding transition in the glass and free ion, respectively. The values of bonding parameter  $b^{1/2}$  are given by

$$b^{1/2} = \left[ \frac{1-\beta'}{2} \right]^{1/2} \quad (10)$$

## Results and Discussion:

### XRD Measurement

Figure 1 presents the XRD pattern of the samples shows no sharp Bragg's peak, but only a broad diffuse hump around low angle region. This is the clear indication of amorphous nature within the resolution limit of XRD instrument.

### Raman spectra

The Raman spectrum of Zinc Lithium Soda lime Cadmium Borosilicate (ZLSLCBS) glass specimens is recorded and is shown in Fig. 2. The spectrum peaks located at 602, 795 and 1204  $\text{cm}^{-1}$ . The band at 602 and 795  $\text{cm}^{-1}$  assigned to Si-O-Si symmetric stretching and bending vibration, respectively. The band at 1204  $\text{cm}^{-1}$  assigned to Si-O-Si asymmetric stretching.

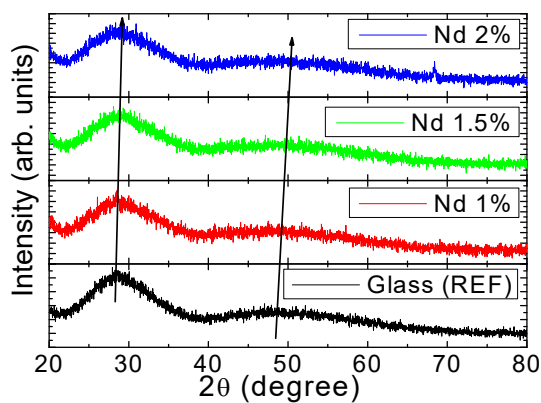


**Fig.1:** X-ray diffraction pattern of  $\text{SiO}_2\text{:ZnO:Li}_2\text{O:CaO:Na}_2\text{O:CdO:B}_2\text{O}_3\text{:Nd}_2\text{O}_3$  glasses.

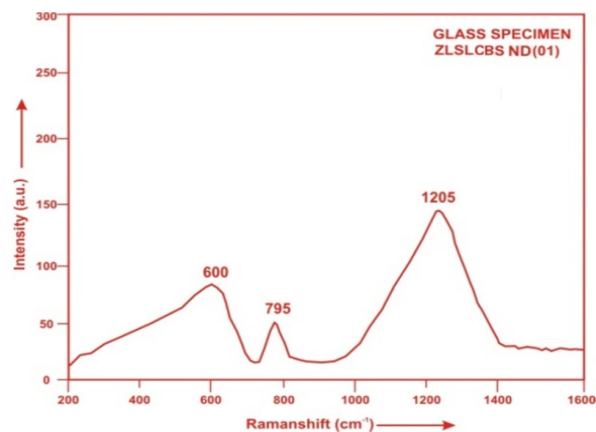


**Fig.2:** Raman spectrum of ZLSLCBSND (01) glass.

### Absorption spectrum

The absorption spectra of ZLSLCBS (ND 01) glass, consists of absorption bands corresponding to the absorptions from the ground state  $^4I_{9/2}$  of  $\text{Nd}^{3+}$  ions. Nine absorption bands have been observed from the ground state  $^4I_{9/2}$  to excited states  $^4F_{3/2}$ ,  $^4F_{5/2}$ ,  $^4F_{7/2}$ ,  $^4F_{9/2}$ ,  $^2H_{11/2}$ ,  $^4G_{5/2}$ ,  $^4G_{7/2}$ ,  $^4G_{9/2}$ , and  $^2G_{9/2}$  for  $\text{Nd}^{3+}$  doped ZLSLCBS(ND 01) glass.

### Excitation Spectrum

The Excitation spectra of  $\text{Nd}^{3+}$  doped ZLSLCBS ND (01) glass specimen has been presented in Figure 4 in terms of Excitation Intensity versus wavelength. The excitation spectrum was recorded in the spectral region 700–1000 nm fluorescence at 1065nm having different excitation band centered at 808 nm and 887 nm are attributed to the ( $^4\text{I}_{9/2} \rightarrow ^4\text{F}_{5/2}$ ) and ( $^4\text{I}_{9/2} \rightarrow ^4\text{F}_{3/2}$ ) transitions, respectively. The highest absorption level is  $^4\text{F}_{5/2}$  and is at 808 nm. So this is to be chosen for excitation wavelength.

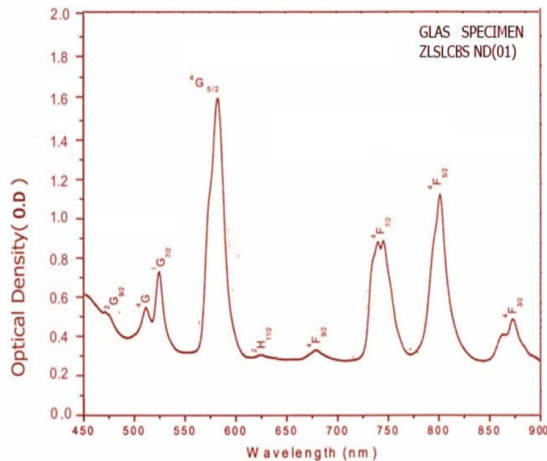


**Fig.3:** Vis-NIR absorption spectra of ZLSLCBS (ND 01) glass.

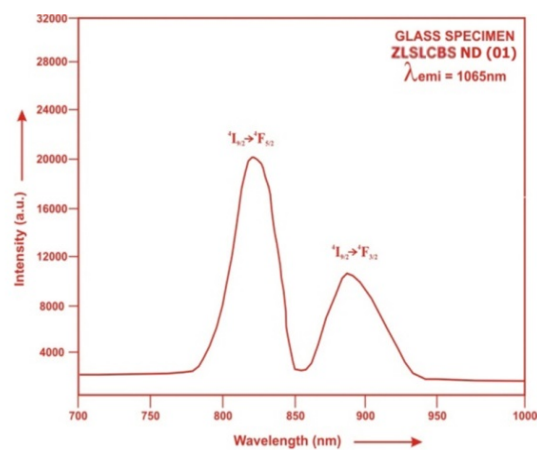


**Fig.4:** Excitation spectra of ZLSLCBSND (01) glass.

The experimental and calculated oscillator strengths for  $\text{Nd}^{3+}$  ions in zinc lithium sodalime cadmium borosilicate glasses are given in **Table 2**.

**Table 2:** Measured and calculated oscillator strength ( $P^m \times 10^{+6}$ ) of  $\text{Nd}^{3+}$  ions in ZLSLCBS glasses.

Energy level from	Glass ZLSLCBS (ND01)		Glass ZLSLCBS (ND1.5)		Glass ZLSLCBS (ND02)	
	$P_{\text{exp.}}$	$P_{\text{cal.}}$	$P_{\text{exp.}}$	$P_{\text{cal.}}$	$P_{\text{exp.}}$	$P_{\text{cal.}}$
$^4\text{I}_{9/2}$						
$^4\text{F}_{3/2}$	4.38	4.03	3.42	3.38	2.64	2.76
$^4\text{F}_{5/2}$	8.24	8.51	7.44	7.46	6.44	6.44
$^4\text{F}_{7/2}$	8.94	9.03	7.83	8.14	6.73	7.26
$^4\text{F}_{9/2}$	0.64	0.51	0.55	0.45	0.43	0.40
$^2\text{H}_{11/2}$	0.24	0.15	0.21	0.13	0.12	0.11
$^4\text{G}_{5/2}$	25.43	25.62	24.33	24.58	23.28	23.70
$^4\text{G}_{7/2}$	4.68	5.44	3.89	4.81	2.63	4.21
$^4\text{G}_{9/2}$	2.83	2.39	2.25	2.05	1.43	1.73
$^2\text{G}_{9/2}$	0.94	3.12	0.82	2.64	0.62	2.19
R.m.s.deviation	0.8009		0.6981		0.7811	

The various energy interaction parameters like Slater-Condon parameters  $F_k$  ( $k=2, 4, 6$ ), Lande's parameter  $\xi_{4f}$ , Racah parameters  $E^k$  ( $k=1, 2, 3$ ), nephelauxetic ratio and bonding parameter for  $\text{Nd}^{3+}$  doped ZLSLCBS glass specimens are given in **Table 3**.

**Table 3:** Computed values of Slater-Condon, Lande', Racah, nephelauxetic ratio and bonding parameter for Nd<sup>3+</sup> doped ZLSLCBS glass specimens.

Parameter	Free ion	ZLSLCBS (ND01)	ZLSLCBS (ND1.5)	ZLSLCBS (ND02)
F <sub>2</sub> (cm <sup>-1</sup> )	331.16	327.29	327.17	327.23
F <sub>4</sub> (cm <sup>-1</sup> )	50.71	49.91	49.94	49.93
F <sub>6</sub> (cm <sup>-1</sup> )	5.154	5.137	5.131	5.134
ξ <sub>4f</sub> (cm <sup>-1</sup> )	884.0	889.48	889.35	889.23
E <sup>1</sup> (cm <sup>-1</sup> )	5024.0	4969.20	4967.90	4968.78
E <sup>2</sup> (cm <sup>-1</sup> )	23.90	23.73	23.69	23.71
E <sup>3</sup> (cm <sup>-1</sup> )	497.0	489.48	489.51	489.50
F <sub>4</sub> /F <sub>2</sub>	0.1531	0.1525	0.1526	0.1526
F <sub>6</sub> /F <sub>2</sub>	0.0155	1.569	0.01568	0.01569
E <sup>1</sup> /E <sup>3</sup>	10.1086	10.16	10.15	10.15
E <sup>2</sup> /E <sup>3</sup>	0.0481	0.0485	0.00484	0.00484
β'		0.98832	0.98796	0.988135
		0.0076398	0.0077583	0.0077024
b <sup>1/2</sup>				

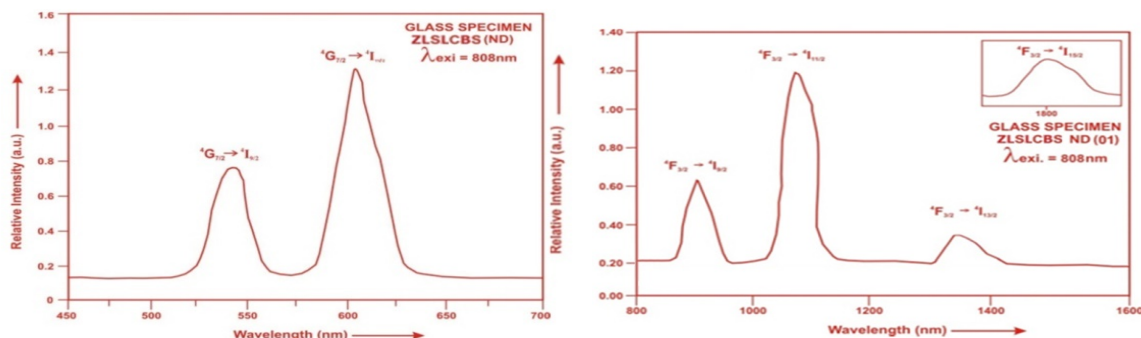
Judd-Ofelt intensity parameters  $\Omega_\lambda$  ( $\lambda = 2, 4$  and  $6$ ) were calculated by using the fitting approximation of the experimental oscillator strengths to the calculated oscillator strengths with respect to their electric dipole contributions. In the present case the three  $\Omega_\lambda$  parameters follow the trend  $\Omega_2 < \Omega_6 < \Omega_4$ . The values of Judd-Ofelt intensity parameters are given in **Table 4**.

**Table 4:** Judd-Ofelt intensity parameters for Nd<sup>3+</sup> doped ZLSLCBS glass specimens.

Glass Specimen	$\Omega_2$ (pm <sup>2</sup> )	$\Omega_4$ (pm <sup>2</sup> )	$\Omega_6$ (pm <sup>2</sup> )	$\Omega_4/\Omega_6$
ZLSLCBS(ND01)	1.718	7.945	2.848	3.204
ZLSLCBS(ND1.5)	2.401	6.617	2.607	2.538
ZLSLCBS(ND02)	3.092	5.339	2.367	2.256

### Fluorescence Spectrum

The fluorescence spectrum of Nd<sup>3+</sup> doped in zinc lithium sodalime cadmium borosilicate glass is shown in Figure 5. There are six broad bands (<sup>4</sup>G<sub>7/2</sub>→<sup>4</sup>I<sub>9/2</sub>), (<sup>4</sup>G<sub>7/2</sub>→<sup>4</sup>I<sub>11/2</sub>), (<sup>4</sup>F<sub>3/2</sub>→<sup>4</sup>I<sub>9/2</sub>), (<sup>4</sup>F<sub>3/2</sub>→<sup>4</sup>I<sub>11/2</sub>), (<sup>4</sup>F<sub>3/2</sub>→<sup>4</sup>I<sub>13/2</sub>) and (<sup>4</sup>F<sub>3/2</sub>→<sup>4</sup>I<sub>15/2</sub>) respectively for glass specimens. The wavelengths of these bands along with their assignments are given in **Table 5**.


**Fig.5:** Fluorescence spectra of ZLSLCBSND (01) glass.

## Conclusion:

In the present study, the glass samples of composition  $(35-x)\text{SiO}_2: 10\text{ZnO}: 10\text{Li}_2\text{O}: 10\text{CaO}: 10\text{Na}_2\text{O}: 10\text{CdO}: 15\text{B}_2\text{O}_3: x\text{Nd}_2\text{O}_3$  (where  $x=1, 1.5, 2$  mol %) have been prepared by melt-quenching method. The value of stimulated emission cross-section ( $\sigma_p$ ) is found to be maximum for the transition ( ${}^4\text{F}_{3/2} \rightarrow {}^4\text{I}_{11/2}$ ) for glass ZLSLCBS(ND 01), suggesting that glass ZLSLCBS (ND 01) is better compared to the other two glass systems ZLSLCBS(ND1.5) and ZLSLCBS(ND02). The large stimulated emission cross section in silicate glasses suggests the possibility of utilizing these systems as laser materials.

## References:

- [1] Murthy Goud, K. K., Ramesh C.H. and Rao, B. A. (2017). Up conversion and Spectroscopic Properties of Rare Earth Codoped Lead Borate Glass Matrix. Material Science Research India, 14, 140-145.
- [2] Mohan, S. and Thind, K. S. (2017). Optical and spectroscopic properties of neodymium doped cadmium-sodium borate glasses Opt, Laser Technol. 95, 36-41
- [3] Lin, H., Pun, E.Y.B. and Wang, X.J. et al. (2005). Intense visible fluorescence and energy transfer in  $\text{Dy}^{3+}$ ,  $\text{Tb}^{3+}$ ,  $\text{Sm}^{3+}$  and  $\text{Eu}^{3+}$  doped rare-earth borate glasses. J. Alloy. Compd., 390, 197-201.
- [4] Ramteke, D.D., Annapurna, K., Deshpande, V.K. and Gedam, R.S. (2014). Effect of  $\text{Nd}^{3+}$  on spectroscopic properties of lithium borate glasses. J. Rare Earths 32(12), 1148-1153
- [5] Karthikeyan, B. and Mohan, S. (2003). Structural, optical and glass transition studies on  $\text{Nd}^{3+}$ -doped lead bismuth borate glasses, Physica B, 334, 298-302.
- [6] Verma, B.R., Baghel, R.N. (2017). Structural and optical properties of  $\text{Eu}^{3+}$  doped silicate phosphors, Indian Journal of Pure Applied Physics, 13, 477-483
- [7] Yasukevich, A. S., Rachkovskaya, G.E., Zakharen, G.B., Trusova, E.E., Kornienko, A. A., Dunina, E.B., Kisel, V. E. and Kuleshov, N. V. (2020). Spectral luminescence properties of oxyfluoride lead silicate germanate glass doped with  $\text{Tm}^{2+}$  ions, Journal of luminescence, 117667.
- [8] Monisha, M., Nancy, A., Souza, D., Nimitha, V. L., Prabhu, S and Sayyed, M.I. (2020).  $\text{Dy}^{3+}$  doped  $\text{SiO}_2\text{-B}_2\text{O}_3\text{-Al}_2\text{O}_3\text{-NaF-ZnF}_2$  glasses: An exploration of optical and gamma radiation shielding features, Current Applied Physics 20(11), 1207-1210.
- [9] Chimalawong, P., Kaewkhao, J., Kedkaew, C. and Limsuwan, P. (2010). Optical and Electronic Polarizability Investigation of  $\text{Nd}^{3+}$ -Doped Soda-Lime Silicate Glasses. Journal of Physics and Chemistry of Solids, 71, 970.
- [10] Rao, T.G.V.M., Kumar, A. R., Neeraja, K., Veeraiyah, N. and Reddy, M.R. (2013). Optical and structural investigation of  $\text{Eu}^{3+}$  ions in  $\text{Nd}^{3+}$  co-doped magnesium lead borosilicate glasses, J. Alloy. Compd. 557, 209-217.
- [11] Berneschi, S., Bettinelli, M., Brenci, M., Dall'igna, R., Nunzi Conti, G., Pelli, S., Profilo, B., Sebastiani, S., Speghini, A. and Righini, G.C. (2006). Optical and spectroscopic properties of soda-lime alumino silicate glasses doped with  $\text{Er}^{3+}$  and/or  $\text{Yb}^{3+}$ , Optical Materials 28, 1271-1275
- [12] Li, H. Z., Xin, Y. S., Hua Mao, Ri, H. Chen, Hao, Jun Zhang, Zhi. and Tai Zhao, Jing (2014). Luminescence properties of  $\text{Ce}^{3+}$ -doped lithium borophosphate glasses and their correlations with the optical basicity, Journal of Non-Crystalline Solids 403, 1-4.
- [13] Sharma, Y.K., Tandon, S.P. and Surana, S.S.L. (2000). Laser action in praseodymium doped zinc chloride borophosphate glasses. Materials Science and Engineering B77, 167-171.

- [14] Gedam, R. S. and Ramteke, D. D. (2013). Influence of CeO<sub>2</sub> addition on the electrical and optical properties of lithium borate glasses, *J. Phys. Chem. Solids* 74, 1399-1402.
- [15] Weber, M.J. (1990). Science and technology of laser glass. *J. Non-Cryst. Solids*, 123, 208–222.
- [16] Dousti, M.R., Poirier, G.Y. and de Camargo, A.S.S., (2020). Tungsten Sodium Phosphate glasses doped with trivalent rare earth ions (Eu<sup>3+</sup>, Tb<sup>3+</sup>, Nd<sup>3+</sup>, Er<sup>3+</sup>) for visible and near infrared applications, *Journal of Non-Crystalline Solids* 530, 119838.
- [17] Reddy, M. S., Uchil, J., Reddy, C. N. (2014). Thermal and Optical properties of Sodium-Phospho-Zinc-Neodymium oxide glass system, *Journal of Advanced Scientific Research*, 5(2), 32-39.
- [18] Manasa, P., Srihari, T., Basavapoorima, C., Joshi, A. S. and Jayasankar, C.K. (2019). Spectroscopic investigations of Nd<sup>3+</sup> ions in niobium phosphate glasses for laser applications. *J. Lumin.* 211, 233–42.
- [19] Vighnesh, K.R., Ramya, B., Nimitha, S., Wagh, A., Sayyed, M.I., Sakar, E., Yakout, H.A. and Dahshan, A. (2020). Structural, optical, thermal, mechanical, morphological and radiation shielding parameters of Pr<sup>3+</sup> doped ZAIFB glass systems, *optical materials* 99, 109512.
- [20] Campbell, J.H., Suratwala, T.I. (2000). Nd<sup>3+</sup>-doped phosphate glasses for high-energy/high-peak-power lasers. *J. Non-Cryst. Solids*, 263, 318–341.
- [21] Gorller-Walrand, C. and Binnemans, K. (1988) Spectral Intensities of f-f Transition. In: Gshneidner Jr., K.A. and Eyring, L., Eds., *Handbook on the Physics and Chemistry of Rare Earths*, Vol. 25, Chap. 167, North-Holland, Amsterdam, 101.
- [22] Sharma, Y.K., Surana, S.S.L. and Singh, R.K. (2009). Spectroscopic Investigations and Luminescence Spectra of Sm<sup>3+</sup> Doped Soda Lime Silicate Glasses. *Journal of Rare Earths*, 27, 773.
- [23] Judd, B.R. (1962). Optical Absorption Intensities of Rare Earth Ions. *Physical Review*, 127, 750.
- [24] Ofelt, G.S. (1962). Intensities of Crystal Spectra of Rare Earth Ions. *The Journal of Chemical Physics*, 37, 511.
- [25] Sinha, S.P. (1983). *Systematics and properties of lanthanides*, Reidel, Dordrecht.
- [26] Krupke, W.F. (1974). Induced-emission cross-section in neodymium laser glasses. *IEEE J. Quantum electron* QE-10, 450-457.

**Table 5:** Emission peak wave lengths ( $\lambda_p$ ), radiative transition probability ( $A_{rad}$ ), branching ratio ( $\beta$ ), stimulated emission cross-section ( $\sigma_p$ ) and radiative life time ( $\tau_R$ ) for various transitions in  $Ho^{3+}$  doped ZLCBS glasses.

Transition	ZLCBS (ND 01)					ZLCBS (ND1.5)				ZLCBS (ND 02)			
	$\lambda_{max}$ (nm)	$A_{rad}(s^{-1})$	$\beta$	$\sigma_p$ ( $10^{-20}$ $cm^2$ )	$\tau_R(\mu s)$	$A_{rad}(s^{-1})$	$\beta$	$\sigma_p$ ( $10^{-20}$ $cm^2$ )	$\tau_R(\mu s)$	$A_{rad}(s^{-1})$	$\beta$	$\sigma_p(10^{-20}$ $cm^2$ )	$\tau_R(10^{-20}$ $cm^2$ )
$^4G_{7/2} \rightarrow ^4I_{9/2}$	532	3877.10	0.4422	0.494	115.22	3384.80	0.4207	0.458	124.30	2956.54	0.3965	0.414	134.10
$^4G_{7/2} \rightarrow ^4I_{11/2}$	595	3263.30	0.3799	1.144		3309.47	0.4114	1.231		3370.14	0.4519	1.327	
$^4F_{3/2} \rightarrow ^4I_{9/2}$	905	983.69	0.1133	0.866		827.30	0.1028	0.746		676.07	0.0907	0.631	
$^4F_{3/2} \rightarrow ^4I_{11/2}$	1075	517.28	0.0596	2.174		452.94	0.0563	2.035		389.94	0.0523	1.884	
$^4F_{3/2} \rightarrow ^4I_{13/2}$	1320	75.39	0.00869	0.378		69.13	0.0085	0.366		62.89	0.0084	0.345	
$^4F_{3/2} \rightarrow ^4I_{15/2}$	1800	1.80	0.0002	0.0224		1.65	0.0002	0.0209		1.50	0.0002	0.0194	